Journal of Alloys and Compounds 500 (2010) 82–86

Contents lists available at ScienceDirect

Journal of Alloys and Compounds

journal homepage: www.elsevier.com/locate/jallcom

Effects of substrate temperatures on the crystallizations and microstructures of electron beam evaporation YSZ thin films

Hong-Hsin Huang [a], Chien-Chen Diao [b], Cheng-Fu Yang [c,*], Chien-Jung Huang [d]

[a] Department of Electrical Engineering, Cheng Shiu University, Kaohsiung, Taiwan, ROC
[b] Department of Electronic Engineering, Kao Yuan University, Kaohsiung, Taiwan, ROC
[c] Department of Chemical and Materials Engineering, National University of Kaohsiung, Kaohsiung, Taiwan, ROC
[d] Department of Applied Physics, National University of Kaohsiung, Kaohsiung, Taiwan, ROC

ARTICLE INFO

Article history:
Received 10 February 2010
Received in revised form 21 March 2010
Accepted 25 March 2010
Available online 2 April 2010

Keywords:
YSZ
Substrate temperature
E-beam evaporation
Textured structure

ABSTRACT

Yttria-stabilized zirconia (YSZ) thin films were grown on Si(1 0 0) substrate using electron beam (E-beam) evaporation by changing the substrate temperature from room temperature (RT) to 250 °C. Effects of different substrate temperatures on the crystalline structure, the lattice constant, the grain growth, and the strain of YSZ thin films and the thickness of interfacial SiO_x layer between Si wafer and YSZ thin films were developed. Even depositing at room temperature, X-ray diffraction (XRD) analyses showed that the reflection peaks of (1 1 1), (2 0 0), (2 2 0), and (3 1 1) planes were formed. The relative reflection intensities of (1 1 1), (2 0 0), (2 2 0), and (3 1 1) planes were changed as the different substrate temperatures were used. The strains of YSZ thin films increased with increasing substrate temperature and reached a minimum value at 200 °C. The amorphous interlayer formed between Si wafer and YSZ thin films and the images of lattice mismatch were also analyzed by using high resolution transmission electron microscopy (HRTEM).

© 2010 Elsevier B.V. All rights reserved.

1. Introduction

Solid oxide fuel cell (SOFC) was a friendly low pollution energy conversion device that could convert the energy of a chemical reaction directly into electrical energy [1]. Yttria-stabilized zirconia, YSZ, had widely been used as an electrolyte in SOFC stack [2–4]. Except the single-layer YSZ thin film, many YSZ-based multi-layer thin films were also developed for the different applications of SOFC devices, for example, Ni-$Sm_{0.2}Ce_{0.8}O_{1.9}$ anode-supported YSZ electrolyte films [5], double layer thermal barrier coating $La_2Zr_2O_7$–YSZ thin films [6], $Ni_{1-x}Fe_xO$–YSZ thin films for intermediate temperature anode [7], and $La_{0.7}Ca_{0.3}CrO_{3-\delta}$–YSZ for the simple SOFCs [1]. Except the Y_2O_3 was used to stabilize the zirconia (ZrO_2) [8,9], other oxides were also added into YSZ to develop their properties, for example, La_2O_3 in YSZ [10] and Sm-doped CeO_2 in NiO/YSZ anode [11]. At the same time, YSZ thin films prepared onto Si substrate had many potential applications, such as buffer layer for epitaxial growth of oxide electrode [12], superconductors [13], and capacitors [14]. To integrate those oxide hetero-structures on Si was very important since current semiconductor and integrated device technologies heavily relied on the depositing technologies of thin films. For that, many different thin film processing techniques were developed to prepare single-layer YSZ thin film or multi-layer YSZ-based thin films, such as ion-beam sputtering, RF sputtering, electrophoretic deposition, electrostatic spray deposition, pulsed laser deposition, and metal organic chemical vapor deposition. Significantly, electron beam (E-beam) evaporation [15,16] offered two major advantages for the thin film deposition. First, a high density power was used as the power source and an easy thickness control was achieved on the depositing rates. And second, the surface area of deposited thin films showed a high temperature, hence, the deposited thin films would crystallize as the substrate was not heated.

E-beam evaporation represented a realizable fabrication technique in that it was based on a molecular deposition of components, thus leading to continuous thin film orientation. Moreover, metallurgical reactions between substrate and source materials leading to thin film contamination were therefore minimized. The orientation of YSZ thin films strongly depended on the depositing parameters and nucleation-heated methods during the depositing processes [17–19] and, further, influenced their applications. In this study, we would use the E-beam evaporation to deposit YSZ thin films on Si(1 0 0) and investigate the effects of substrate temperature on the characteristics of YSZ thin films. For E-beam evaporation, the effects of Y_2O_3 content on the grown and structural characteristics of YSZ thin films prepared at 200 °C had been reported by Wu et al. [15] and Hartmanova et al. [16]. However, they did not study the effects of substrate temperatures on the growth

* Corresponding author. Tel.: +886 7 5919283; fax: +886 7 5919277.
E-mail address: cfyang@nuk.edu.tw (C.-F. Yang).

0925-8388/$ – see front matter © 2010 Elsevier B.V. All rights reserved.
doi:10.1016/j.jallcom.2010.03.216

characteristics in detail. Suh et al. [20] indicated the substrate temperatures had large influences on the crystalline orientations of deposited thin films and the formations of interfacial layers. We had found that even the substrate was unheated, the orientation peaks of YSZ thin films were formed. We would show that the substrate temperature played an important role in nucleation and relatively crystalline intensities of orientations in YSZ thin films. We would also show that the substrate temperature had large influences on the lattice constants and strains of YSZ thin films. High resolution transmission electron microscopy (HRTEM) was used to analyze the lattice defects and the variations of interfacial layers. We could use the analyzed data to demonstrate the phenomena for the variations of crystallization of YSZ thin films and to find the thickness of interfacial layer between the YSZ thin films and Si(1 0 0) substrate.

2. Experimental procedures

YSZ polycrystal, zirconia with 8 mol% Y_2O_3, with purity higher than 99.9% was synthesized from a powder supplied by Tosoh Co. Ltd., Tokyo, Japan. In order to obtain the disks used as the source material for E-beam evaporation, the powder was pressed and sintered at 1400 °C for 4 h. The Si(1 0 0) substrate was cleaned in isopropyl alcohol (EPA) and deionized water and dried by nitrogen gas. A vacuum system with 5×10^{-6} Torr was used as base pressure and for deposition, oxygen was introduced into the chamber to adjust the working pressure of 1×10^{-5} Torr. During the depositing process, substrate was hold with a working distance of 20 cm and heated by irradiation at 100 °C, 150 °C, 200 °C, and 250 °C, respectively. The deposition rate of YSZ thin films was controlled by the power of E-beam and monitored by a thickness control system (CRTM-6000, ULVAC, Japan). The crystalline structure of YSZ thin films was identified by XRD with Cu Kα. The thickness and surface observation of YSZ thin films were characterized by field emission scanning electron microscopy (FESEM) and the micro structural analyses were done using HRTEM.

3. Results and discussion

The thicknesses of YSZ thin films deposited under different substrate temperatures are observed from the cross-section images of FESEM and the results are shown in Fig. 1, the thicknesses for all samples are about 500 nm. As the cross micrographs shown in Fig. 1 are compared, there are different results as the substrate temperature is changed. As the substrate temperature increases from RT to 200 °C, the YSZ thin films grow like a bar or a disk along the up direction. But depositing at 250 °C, the bar- or disk-shaped growths are transformed into the handstand-triangle disk. Fig. 1 also shows that the interfacial layers (the SiO_x layer shown in Fig. 5) between YSZ thin films and Si substrate become un-apparently as the substrate temperature increases. Those results suggest that the YSZ thin films have differently crystalline orientation and leading to different texture coefficients, that will be shown in Figs. 2 and 3. Also, the substrate temperature has large influences on the characteristics of epitaxial growth YSZ thin films and the interfacial layer.

The XRD patterns of YSZ thin films on Si(1 0 0) substrate deposited under different substrate temperatures are shown in Fig. 2. The reflection peaks of (1 1 1), (2 0 0), (2 2 0), and (3 1 1) planes are found in all YSZ thin films and the crystalline YSZ fluorite structure is obtained, even without external heating is used. In general, the mobile energy of YSZ thin films is highly dependent on the depositing parameters. For that, the orientation of YSZ thin films also strongly depends on the substrate condition used during the depositing processes, especially on the substrate temperature. Because lower substrate temperature means lower mobile energy supplied for absorbed species and amorphous thin films are obtained [21]. However, the crystalline YSZ thin films are obtained and the reflection intensity of (2 2 0) plane obviously increases with increasing substrate temperature. In case of YSZ thin films, the (1 1 1) plane has the lowest surface energy. Thus, preferential (1 1 1) out-of-plane orientation is developed under the substrate temperature of 250 °C and the YSZ thin film has the different grain growth shape or direction, as the cross morphologies shown in Fig. 1.

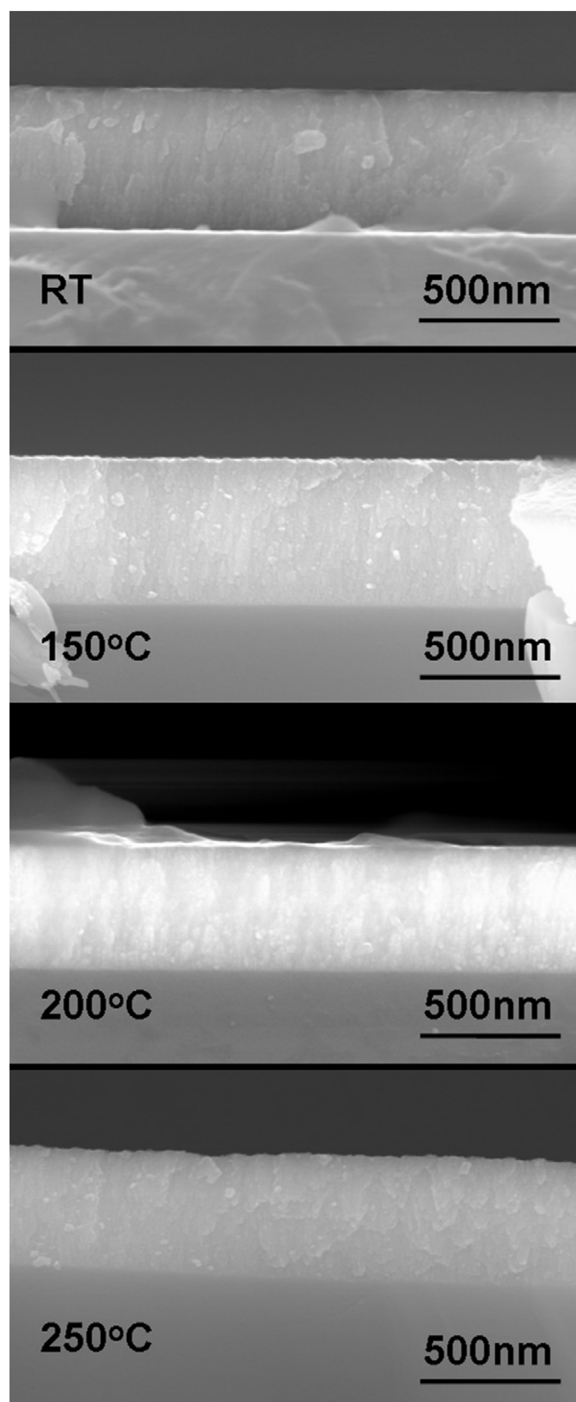

Fig. 1. Cross-section images of YSZ thin films deposited under different substrate temperatures.

In Fig. 2, the reflection intensity of (2 0 0) plane reveals a maximum value at 200 °C. Crystallographic texture of YSZ thin films is referred and texture coefficient (TC) is used to describe the textures of thin films with Eq. (1) [22]:

$$TC_{h\,kl} = \frac{I_{hkl}/I^o_{hkl}}{1/n \sum I_{hkl}/I^o_{hkl}} \quad (1)$$

where I_{hkl} is reflection intensity of (hkl), I^o_{hkl} is standard reflection intensity of (hkl) reported in JCPDs card (No. 82-1246), n is number of reflection peaks. The TC values of various reflections of YSZ thin films shown in Fig. 3 indicate that the (2 0 0) plane pos-

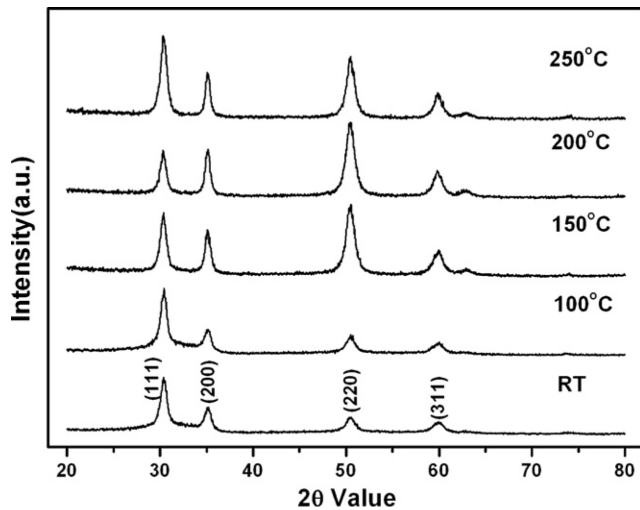

Fig. 2. The XRD patterns of YSZ thin films deposited under different substrate temperatures.

sesses the highest TC value at the substrate temperature range of RT ~ 150 °C. Although the TC value of (2 0 0) plane slightly decreases with increasing depositing temperature, it still reveals a high TC value at the substrate temperature range of 200–250 °C. For ZrO_2 with 8 mol% Y_2O_3, the cubic phase is more stable and (2 0 0) plane is preferred growing orientation on Si(1 0 0). It agrees with the report of Wu et al. [15] who pointed out the maximum diffraction peak was in the crystalline (2 0 0) plane for YSZ thin film with 7 mol% Y_2O_3 deposited at 350 °C. Park et al. [23] reported that YSZ deposited on various Ni substrates, resulting in the films with either mixtures of (1 1 1) and (0 0 2) planes or mostly (1 1 1) plane. Hata et al. [24] prepared YSZ thin films on Si(1 0 0), Si(1 1 0), and Si(1 1 1) substrates by RF sputtering and concluded that YSZ orientation was properly controlled by substrate surface in the cases of Si(1 0 0) and Si(1 1 1). Hata et al. [24] also showed a lattice model to demonstrate that the plane of YSZ (2 0 0) was the dominated orientation on Si(1 0 0) substrate which agrees with our results shown in Figs. 2 and 3. Nevertheless, the (3 1 1) plane with the lowest TC value may be confined by the Si(1 0 0) according to the prediction of atomic model of Hata et al.

The morphologies of YSZ thin films prepared are shown in Fig. 4 as a function of substrate temperature, the smooth surface is

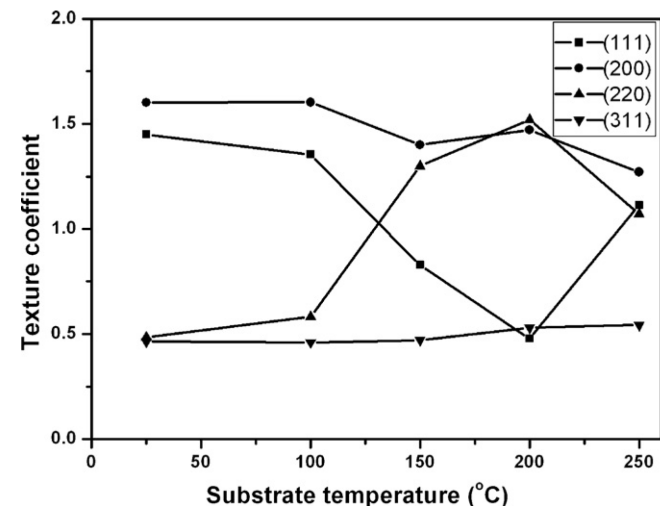

Fig. 3. The texture coefficients of YSZ thin films deposited under different substrate temperatures.

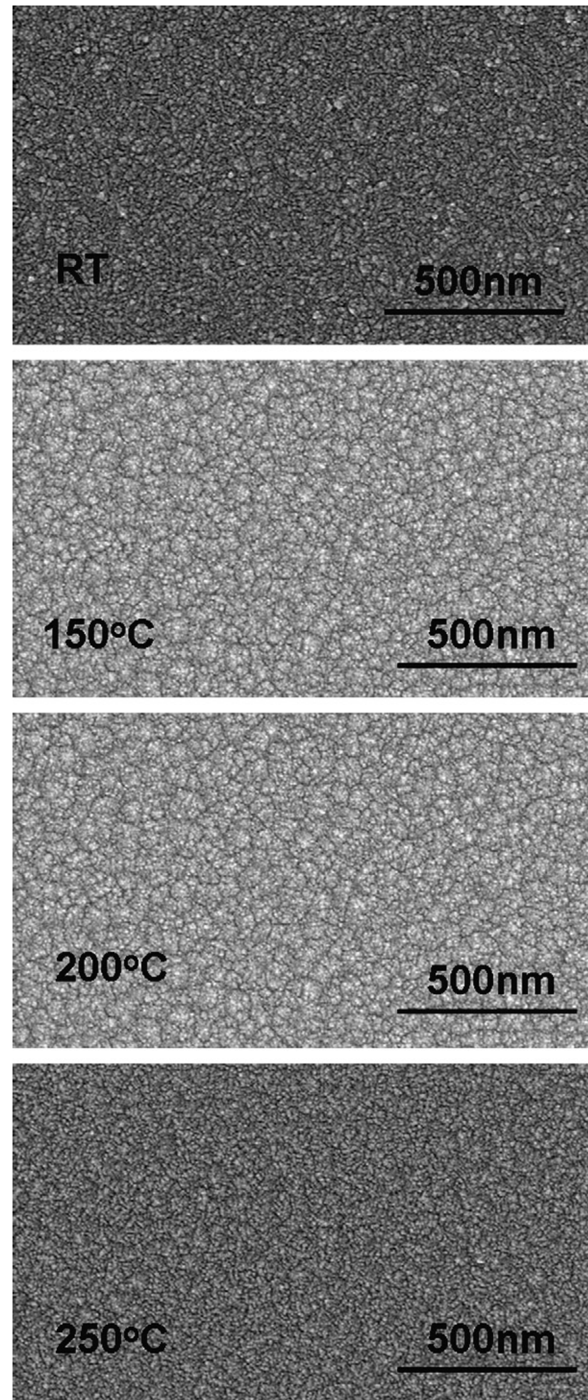

Fig. 4. Surface observations of YSZ thin films deposited under different substrate temperatures.

obtained at higher temperature. For higher depositing temperature, the species absorbed onto the substrate possesses higher mobile energy to move toward the lower energy site resulting in more smooth morphologies obtained. However, the variations of grain sizes are dependent on the substrate temperature and are not easily calculated from the surface observation. We will illustrate the variations of grain sizes from the X-ray patterns in Fig. 5.

Thin films always induce the internal stress, which might mislead in determining the lattice parameters from one reflection when the coatings are under stress. The relationship between lattice strain (η) and full width at half maximum value (FWHM, β) can

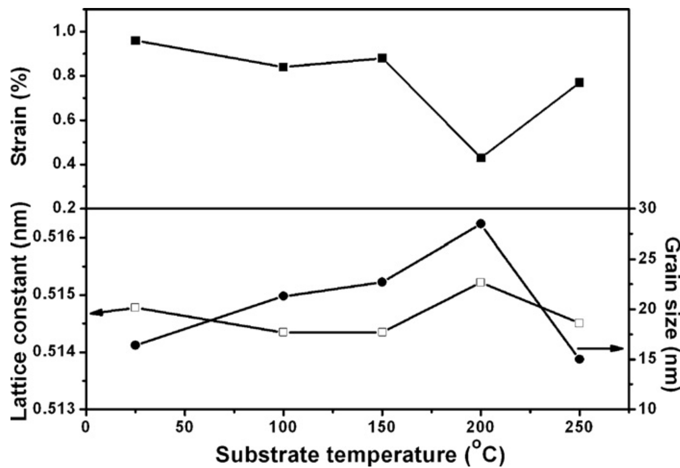

Fig. 5. The lattice constants, grain sizes, and strains of YSZ thin films deposited under different substrate temperatures.

be expressed as Eq. (4) [25]:

$$\frac{\beta \cos\theta}{\lambda} = \frac{2\eta \sin\theta}{\lambda + 1/d} \quad (2)$$

where θ is a Bragg's angle, λ is wavelength of X-ray, and d is crystallite size. For a XRD profile with more than 2 diffraction peaks, the 2η and $1/d$ can be separately obtained by calculating the slope and intercept of profile of $\sin\theta/\lambda$ versus $\beta\cos\theta/\lambda$. Fig. 4 shows the dependences of grain size, lattice constant, and strain on substrate temperatures illustrated from Eq. (2). The grain size increases with increasing substrate temperature and reaches the maximum at 200 °C, the results mean that higher temperature has benefit on grain growth. However it dramatically decreases at 250 °C, the phenomena is believed to be caused by the change of mainly crystalline orientation, as shown in Figs. 3 and 4. The strain of YSZ thin films first decreases, reaches a minimum at 200 °C, and then critically increases at 250 °C. The lattice constant reveals a maximum as the substrate temperature is 200 °C, at which the strain has a minimum value. The phenomena are believed to be caused by the variations of mainly crystalline orientations, as shown in Fig. 3. The Nelson–Riley function can be utilized to determine the lattice constants because of the minimizing effect of stress [26]:

$$\frac{\Delta d}{d} = K\left(\frac{\cos^2\theta}{\sin\theta} + \frac{\cos^2\theta}{\theta}\right) \quad (3)$$

where d is plane space, Δd is the difference of plane space, K is a constant, and θ is the diffraction angle. In this method, a better straight line is obtained with the $\cos^2\theta/\sin\theta$, so the following equation is used to obtain the lattice constant:

$$a = a_0 + a_0 K'\left(\frac{\cos^2\theta}{\sin\theta}\right) \quad (4)$$

where a is the calculated lattice constant from the XRD patterns and a_0 is real lattice constant. The lattice constants of YSZ thin films are shown in Fig. 5. At first, the lattice constants slightly decrease with increasing substrate temperature and then critically increase as the substrate temperature is 200 °C. Lattice constants of YSZ thin films deduced from XRD data and Eq. (4) are 0.51435–0.51522 nm. The variations of lattice constants are caused by variations of strains and grain sizes, as shown in Fig. 5. The maximum lattice constant and grain size revealed in 200 °C-deposited YSZ thin films are caused by the strain relaxation.

Fig. 6 shows a cross-sectional HRTEM image of YSZ thin films deposited on Si(1 0 0) substrate. The YSZ thin films grow epitaxially on Si(1 0 0) with the apparently amorphous interfacial SiO_x layer of about 16 nm. This amorphous SiO_x layer is believed to be due to the reaction of the surface of Si wafer with oxygen before the depositing process because we have not conducted any acid-etching process on native Si wafer prior to deposition. The free energy of formation of ZrO_2 ($G_{800\,K} = -941.6$ kJ/kmol) is lower than that of SiO_2 ($G_{800\,K} = -734.2$ kJ/kmol) [23]. Rubloff et al. [27] found that the critical oxygen partial pressure above which silicon oxide layer remained stable at 730 °C was about 7×10^{-5} mbar (5.25×10^{-5} Torr). The partial pressure effect on the growth of YSZ thin films and YSZ buffer multi-layers on Si had also been investigated by Chow and Wang [28]. They reported that no interfacial layer was found when YSZ thin films prepared by PLD under 5×10^{-6} mbar (3.75×10^{-6} Torr), while, interfacial layer with thickness of about 4.5 nm was found under pressure of 5×10^{-4} mbar (3.75×10^{-4} Torr).

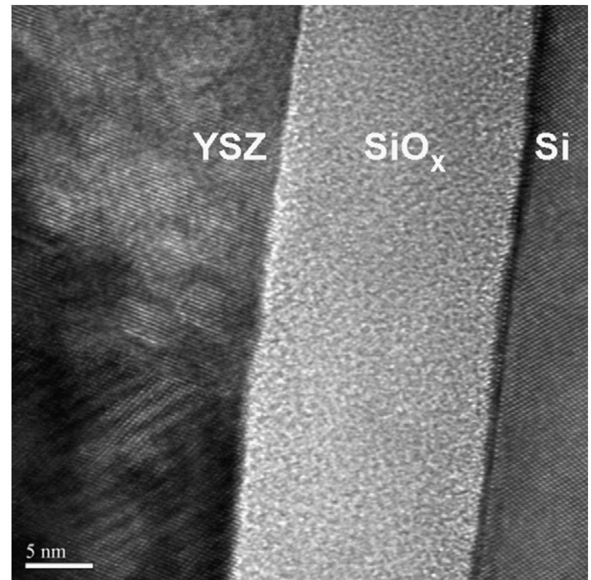

Fig. 6. HRTEM analysis of interface between YSZ and Si substrate.

Those results demonstrate that the substrate temperature and oxygen pressure will influence the thickness of SiO_2 layer and then will influence the crystalline orientation and the TC value of YSZ thin films. Because the free energy of ZrO_2 is lower than that of SiO_2, for that Zr ions have absorbed oxygen ions from SiO_x layer on the surface of Si wafer, reducing SiO_2 to SiO. SiO decomposition is expected for lower oxygen partial pressure, as a result, the thickness of SiO_x layer will be reduced or even eliminated. In our depositing process, the deposition of YSZ thin films is conducted in lower oxygen partial pressure condition (1×10^{-5} Torr). From the observation of HRTEM (not shown here), the thickness of SiO_x layer becomes thinner and the interfacial layer between Si substrate and YSZ thin films is more unapparent (Fig. 1) as higher substrate temperature is used. The decrease in the thickness of SiO_x layer with the increasing substrate temperature is that the oxygen ions absorbing efficiency of Zr ions increases and the interfacial SiO_x layer is reduced. For that, as the substrate temperature increases, a thinner interfacial layer is found by using E-beam evaporation.

Because the SiO_x layer becomes thinner, the YSZ thin films can epitax according to the orientation of Si(1 0 0) wafer and this is the reason that the orientation of (2 0 0) plane of YSZ thin film increases with increasing substrate temperature. To identify the microstructures of deposited YSZ thin films under different substrate temperatures, HRTEM images are taken from the RT-deposited and 200 °C-deposited YSZ thin films and compared in Fig. 7. In Fig. 7, which is taken from the [1 1 1] direction axis, the lat-

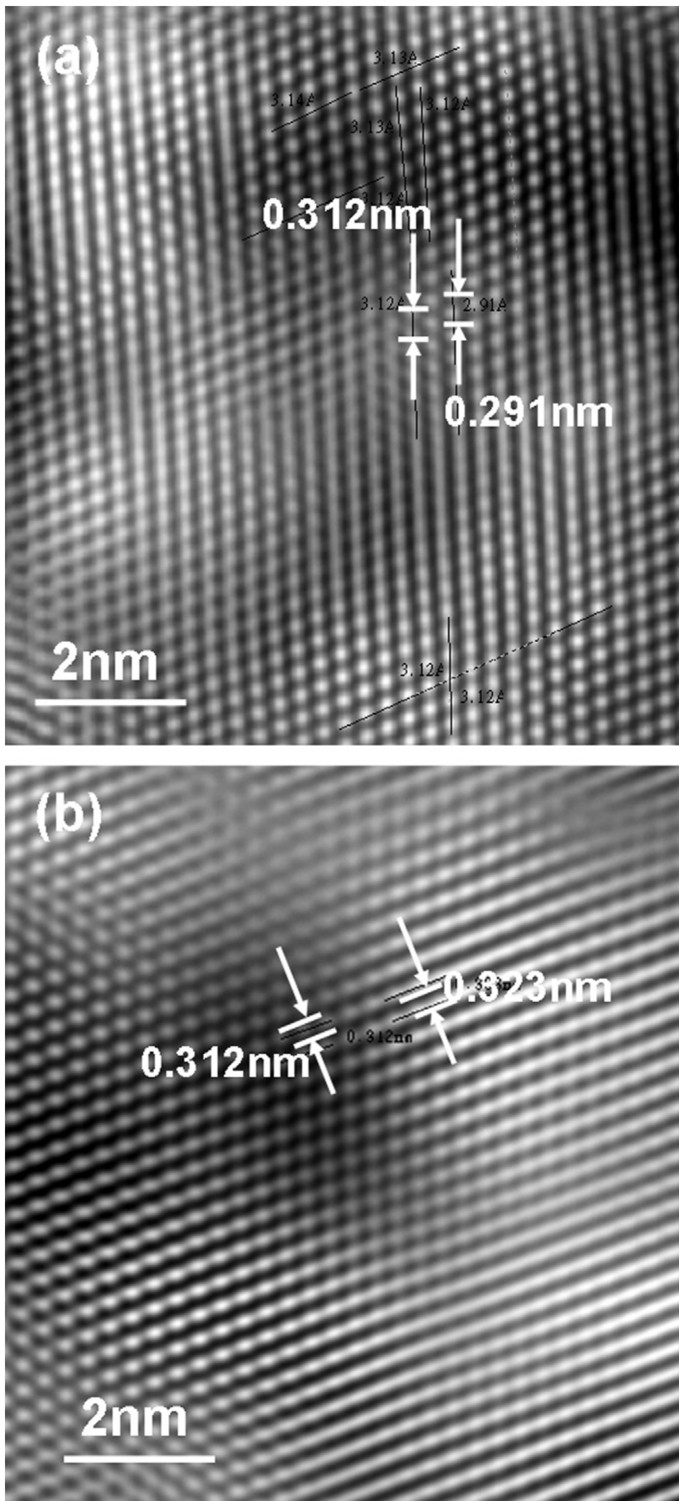

Fig. 7. HRTEM images of YSZ[1 1 1] for substrate temperatures of (a) room temperature and (b) 200 °C.

tice clearly appears cubic and continuation. However, a few lattice distortions and the larger lattice mismatch are apparently observed in the RT-deposited YSZ thin films than in the 200 °C-deposited YSZ thin films.

4. Conclusions

The crystalline YSZ thin film is obtained at RT because the E-beam evaporation emerges enough source energy. The reflection intensity of (2 0 0) plane increases with increasing substrate temperature and reaches a maximum value at 200 °C. The measurements of texture coefficients (TC) indicate that the (2 0 0) plane possesses the highest TC value at the temperature range of room temperature ∼250 °C. Lattice constants of deposited YSZ thin films deduced from XRD data and Nelson–Riley function are 0.51435–0.51522 nm. As the substrate temperature increases, the grain size first increases, reaches the maximum at 200 °C, and then dramatically decreases at 250 °C. On the other hand, the strain first decreases, reaches a minimum at 200 °C, and then critically increases at 250 °C. The change of mainly crystalline orientation is the phenomena to cause those results. From the observation of HRTEM, the substrate temperature also has large influences on the thickness of SiO_x interfacial layer between Si substrate and YSZ thin films and on the lattice mismatch of epitaxial YSZ thin films.

References

[1] B. Lin, S. Wang, X. Liu, G. Meng, J. Alloys Compd. 490 (2010) 214–222.
[2] L. Jia, Z. Lü, X. Huang, Z. Liu, K. Chen, X. Sha, G. Li, W. Su, J. Alloys Compd. 424 (2006) 299–303.
[3] A. Sanson, P. Pinasco, E. Roncari, J. Eur. Ceram. Soc. 28 (2008) 1221–1226.
[4] H. Yokokawa, N. Sakai, T. Horita, K. Yamaji, M.E. Brito, H. Kishimoto, J. Alloys Compd. 452 (2008) 41–47.
[5] Y. Zhang, X. Huang, Z. Lua, Z. Liu, X. Ge, J. Xu, X. Xin, X. Sha, W. Su, J. Alloys Compd. 428 (2007) 302–306.
[6] Z. Xua, L. He, R. Mu, X. Zhong, Y. Zhang, J. Zhang, X. Caoa, J. Alloys Compd. 473 (2009) 509–515.
[7] J. Ding, J. Liu, W. Guo, J. Alloys Compd. 480 (2009) 286–290.
[8] C.W. Kuo, Y.H. Shen, I.-M. Hung, S.B. Wen, H.E. Leed, M.C. Wang, J. Alloys Compd. 472 (2009) 186–193.
[9] Z.G. Liu, J.H. Ouyang, Y. Zhou, J. Alloys Compd. 473 (2009) L17–L19.
[10] S.J. Hong, S.J. Kim, W.K. Han, S.G. Kang, J. Alloys Compd. 486 (2009) 543–548.
[11] L. Zhang, J. Gao, M. Liu, C. Xia, J. Alloys Compd. 482 (2009) 168–172.
[12] H.N. Lee, D. Hesse, N. Zakharov, U. Gosele, Science 296 (2002) 2006–2009.
[13] J. Xiong, Y. Chen, Y. Qiu, B. Tao, W. Qin, X. Cui, J. Tang, Y. Li, Physica C 454 (2007) 56–60.
[14] S. Jun, Y.S. Kim, J. Lee, Y.W. Kim, Appl. Phys. Lett. 78 (2001) 2542–2544.
[15] S.G. Wu, H.Y. Zhang, G.L. Tian, Z.L. Xia, J.D. Shao, Z.X. Fan, Appl. Surf. Sci. 253 (2006) 1561–1565.
[16] M. Hartmanova, K. Gmucova, M. Jergel, I. Thurzo, F. Kundracik, M. Brunel, Thin Solid Films 345 (1999) 330–337.
[17] K. Yang, J.H. Shen, K.Y. Yang, I.M. Hung, K.Z. Fung, M.C. Wang, J. Alloys Compd. 436 (2007) 351–357.
[18] K. Rodrigo, J. Knudsen, N. Pryds, J. Schou, S. Linderoth, Appl. Surf. Sci. 254 (2007) 1338–1342.
[19] G. Vourlias, N. Pistofidis, P. Psyllaki, E. Pavlidou, G. Stergioudis, K. Chrissafis, J Alloys Compd. 483 (2009) 378–381.
[20] J.H. Suh, S.H. Oh, H.S. Kim, S.Y. Choi, C.G. Park, Vacuum 74 (2004) 423–430.
[21] H.H. Huang, H.P. Chang, Y.T. Chien, M.C. Huang, J.S. Wang, J. Cryst. Growth 287 (2006) 458–462.
[22] C.S. Barrett, T.B. Massalski, Structure of Metals, Pergamon Oxford, New York, 1980, p. 204.
[23] C. Park, D.P. Norton, D.F. Lee, D.T. Verebelyi, A. Goyal, D.K. Christen, J.D. Budai, Physica C 341 (2000) 2481–2482.
[24] T. Hata, K. Sasaki, Y. Ichikawa, K. Sasaki, Vacuum 59 (2000) 381–389.
[25] H.H. Huang, F.Y. Hsiao, N.C. Wu, M.C. Wang, J. Non-Cryst. Solids 351 (2005) 3809–3815.
[26] H.H. Huang, M.H. Hon, M.C. Wang, J. Cryst. Growth 240 (2002) 513–520.
[27] G.W. Rubloff, K. Hofmann, M. Luer, D.R. Young, Phys. Rev. Lett. 58 (1987) 2379–2382.
[28] S.Y. Chow, S. Wang, Ceram. Int. 30 (2004) 1257–1261.